

## Reliability optimization design of electromagnetic proportional directional valve

Hua Zhang

Department of Mechanical Engineering, Anhui Science and Technology University, Fengyang 233100, China

Corresponding Author Email: [chinafeihong@163.com](mailto:chinafeihong@163.com)

**Received:** 18 August 2017  
**Accepted:** 24 February 2018

### ABSTRACT

Insufficient electromagnetic force and too high temperature rise to burnout the coil are the typical faults of the electromagnetic proportional directional valve. The simplified field model used in traditional analysis method has poor accuracy. In this paper, the magnetic field distribution of the valve is modeled and analyzed by using the finite element method. Magnetic force is calculated based on the virtual displacement principle. In addition, the influence laws of the geometry and parameters acting on electromagnetic force are taken into consideration in order to model the coil temperature field of the valve. The influence of coil control current and heat transfer coefficient on the temperature rise of coil is analyzed, which provides a theoretical basis for the reliability optimization design of electromagnetic proportional directional valve.

### Keywords:

*electromagnetic proportional directional valve, electromagnetic force, temperature field, reliability optimization design*

## 1. INTRODUCTION

Electromagnetic proportional directional valve is widely used in electro-hydraulic control systems. For example, the electromagnetic proportional directional valve is applied to control a hydraulic motor power system on flexible intelligent sprayer chassis developed by the author, in this way the chassis speed control and steering functions are realized. It is an essential component of electro-hydraulic control system with high price and failure rate. The typical failures are insufficient electromagnetic force [1] and the overheat of the coil, which lead to the malfunction of the valve core. The traditional analysis method adopts simplified models, which lead to poor analysis accuracy. This method is not suitable for nonlinear and complicated analysis of electromagnetic valves [2]. Mechanical optimization design method emphasizes only on parameters optimization without considering the geometry optimization [3-6]. On the other hand, the finite element method does not require complicated mathematical model but it needs accurate model of the geometry and boundary conditions. Therefore, the finite element method for electromagnetic field and thermal analysis theory are adopted in order to solve the parameters and geometry optimization problem. Moreover, the changing regulation and influence factors of electromagnetic force and the temperature rise of the coil are explored.

## 2. ELECTROMAGNETIC FIELD ANALYSIS OF ELECTROMAGNETIC PROPORTIONAL DIRECTIONAL VALVE

The electromagnetic proportional directional valve adopted in flexible intelligent sprayer chassis is PRM2-06-3Z11.Brand is ARGO-HYTOS. The structure is shown in figure 1.

The electromagnetic proportional directional valve drives the valve core mainly by the electromagnetic force between the electromagnet coil and the armature. The stroke of the valve core is proportional to coil current and the

electromagnetic force changes with the stroke of the valve core [7]. After the current is off, the reset spring is used for resetting the spool. Taking the electromagnet part of the valve as the analysis object, the electromagnet structure diagram is set up, as shown in figure 2.

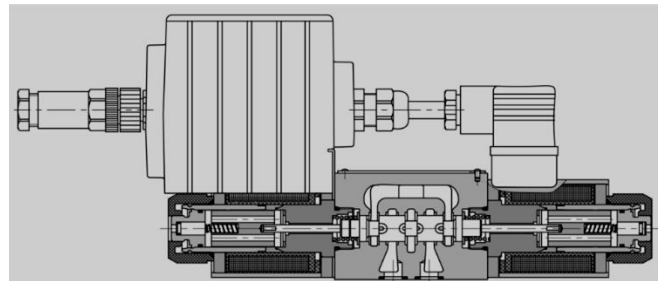
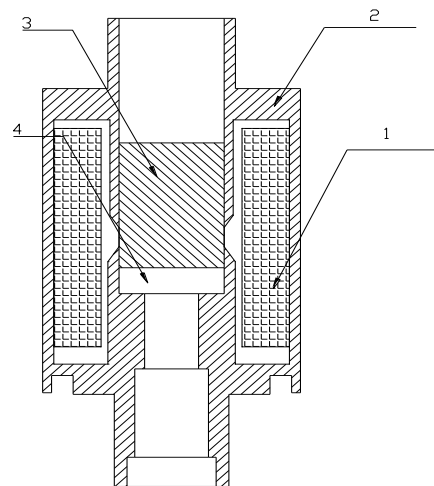


**Figure 1.** Structure of electromagnetic proportional directional valve



1-coil; 2-iron core; 3-armature; 4-air gap

**Figure 2.** Electromagnet structure

Electromagnetic field theory and finite element method are used to analyze the electromagnetic field.

(1) Pre-processing

Since the proportional electromagnets are axisymmetric, the two-dimensional axisymmetric analysis method is used in ANSYS. Only half model is required and the whole model can be obtained by the function **mirror** [8] when modeling. The element type is set as PLANE13. The relative permeability of air and coil is set as 1 and that of iron core and armature is 2000. Half model is divided into quadrilateral mesh, as shown in figure 3.

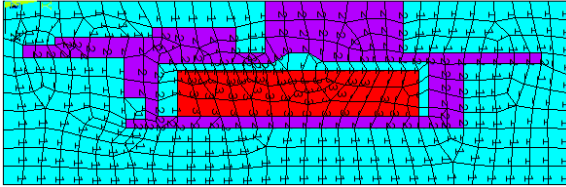


Figure 3. The proportional electromagnet meshing

The armature is defined as an element and a magnetic force boundary condition is added. The current density load is applied to the coil as:

$$J = NI / A_{COIL} \quad (1)$$

where,  $N$ - Coil turns;  $I$ - The current intensity of the coil;  $A_{COIL}$ - Coil cross-sectional area

In this paper, the coil turns of valve are **10000**, the current intensity is 1, the range of current value is 0.004-0.02A and the cross sectional area of the coil is 0.015m \* 0.05m.

Parallel condition of magnetic flux lines is applied to all external nodes.

(2) Solution

Static electromagnetic field analysis solver is used to solve the problem.

(3) Post-processing

View the results of the solution. The solution is shown in figure 4.

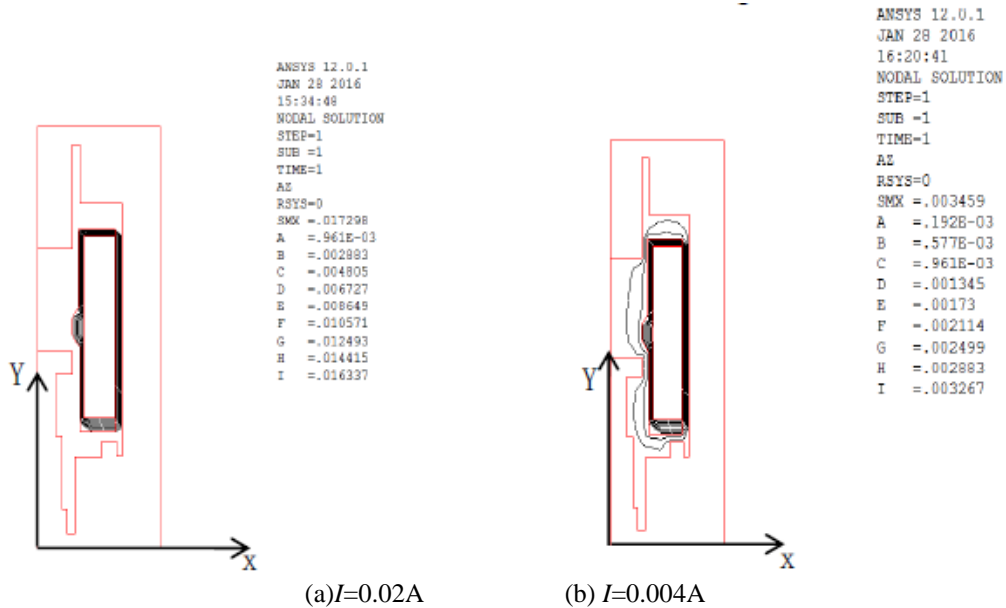


Figure 4. Distribution of magnetic flux lines

The internal magnetic flux tends to be dense with the increase of current intensity. The magnetic flux is mainly distributed in the gap between the coil and the iron core and the armature when the current intensity reaches the maximum value. There are no closed magnetic flux lines through the iron core and the armature, as shown in figure 4(a).

Electromagnetic force is calculated using the principle of virtual displacement:

$$F = \lim_{\Delta x \rightarrow 0} \frac{\Delta W'}{\Delta x} = \frac{dW'}{dx} = - \left[ \left( \frac{E_{x+\Delta x} + E_x}{\Delta x} \right) \right] \quad (2)$$

where,  $\Delta W'$  -The required energy,  $\Delta x$ -Displacement;  $E_x$  - System energy at zero displacement point;  $E_{x+\Delta x}$  - System energy at the expected armature position.

As a result of ANSYS: the electromagnetic force is 40.75N in direction -Y when the coil current is 0.02A. The

electromagnetic force is 0.19966N in direction -Y when the coil current is 0.004A.

(4) Optimization design

Power consumption and electromagnetic force are the two important factors of electromagnetic valve design. Power consumption is reduced usually by changing the coil turns and line diameter while ensuring that the electromagnetic force is sufficient [9]. But the number of turns and the coil diameter have a comprehensive influence on the force and power consumption. The increase of coil turns can increase the electromagnetic force [10], but it will lead to remarkable temperature rise of the coil. This is not positive to improve the reliability of the valve. In addition, the diameter of the coil will also affect the response characteristics of the valve [11]. Therefore, methods are studied to increase electromagnetic force considering coil current and electromagnet geometric dimension.

① Analysis of the influence of different current intensity on electromagnetic force

The electromagnetic force is calculated with the virtual displacement principle in ANSYS under four different coil current intensities, 0.004A, 0.01A, 0.015A and 0.02A. The changing curve is generated as shown in figure 5.

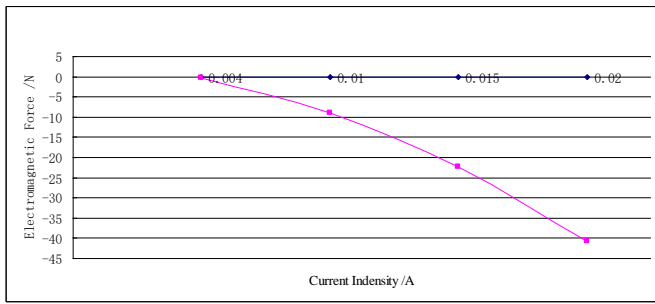
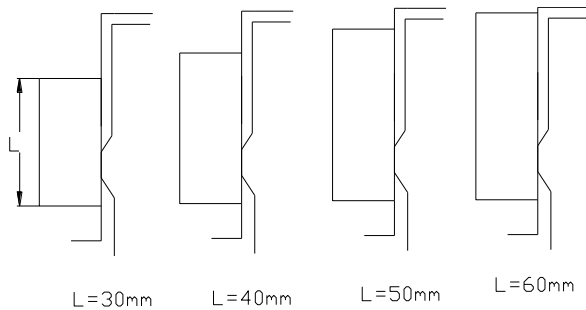


**Figure 5.** Curve of electromagnet force changing with current intensity

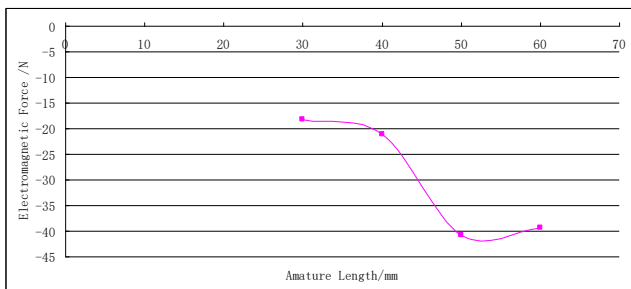
The electromagnetic force of the coil increases linear with the increase of the coil current intensity as shown in figure 5.

② The influence of armature length on electromagnetic force.

30mm, 40mm and 60mm of armature length are selected to compare and analyze the influence of electromagnet length on electromagnetic force in the proximity of the nominal length 50mm. The Different armature lengths are shown in figure 6(a) and their effects on electromagnetic force are shown in figure 6(b).



(a) Different armature length



(b) Changing curve of electromagnet force with armature length

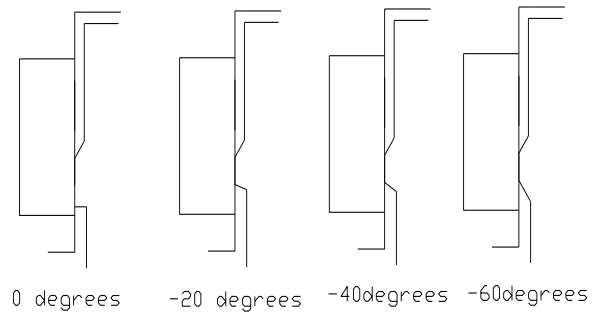
**Figure 6.** Different armature lengths and their effects on electromagnet force

Figure 6(b) shows that with the increase of the armature length, the electromagnetic force increases gradually, but there is a peak value. The force decreases when the armature length

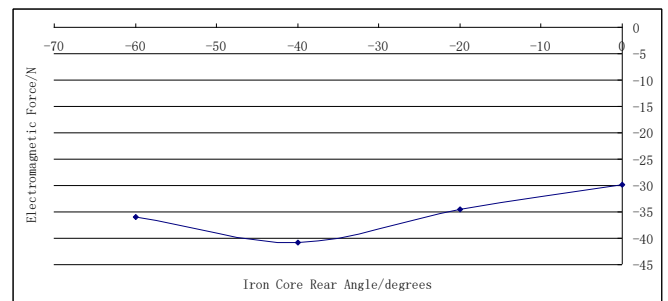
is greater than the nominal length. Therefore, the optimum armature length in range of 30mm-60mm is about 55mm.

③ The influence of the rear angle of the iron core on electromagnetic force

The structure of the electromagnet must be designed as a cone shaped shoe pole structure around the cone [12] in order to realize the proportional relation between the coil current and the electromagnetic force. Therefore, it is necessary to determine the size and geometry of the cup through the optimization design, in which the rear angle of iron core has a greater impact. The rear angles of different iron core are shown in figure 7(a) and the influence of the different rear angles of iron core on electromagnetic force is shown in figure 7(b).



(a) Different rear angles of iron core



(b) Changing curve of electromagnet force with the rear angle of iron core

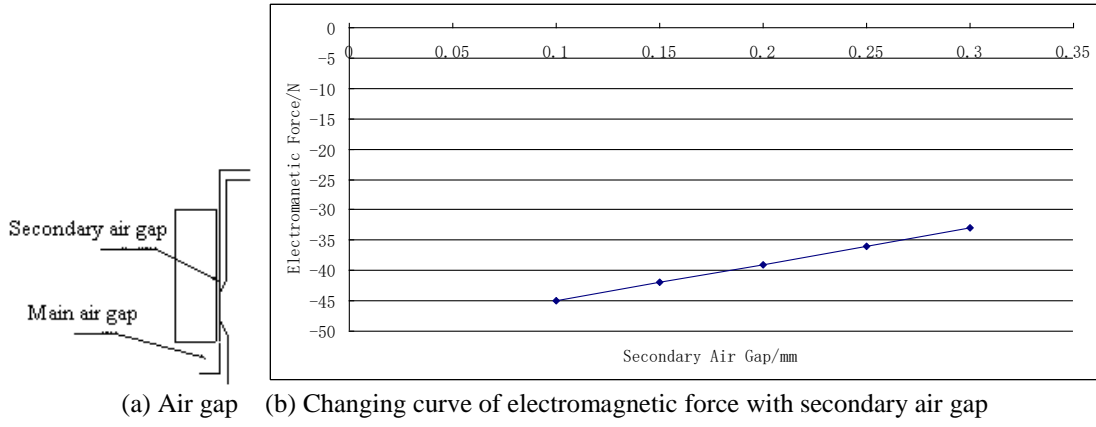
**Figure 7.** Different rear angles of iron core and the effect on electromagnet force

Figure 7(b) shows that the corresponding electromagnetic force increases gradually when the rear angle of the iron core begins to decrease from 0 degrees. The force reaches the maximum value when the rear angle reaches -40 degrees. Crossing through this point, the force decreases as the angle proceeds to decrease. Therefore, the optimum angle of the iron core in the range of -60 – 0 degrees is -40 degrees.

④ The influence of secondary air gap on electromagnetic force

The air gap in the electromagnet has a great influence on performance. The air gap is divided into the main air gap and the secondary air gap, as shown in figure 8(a). The influence of the secondary air gap on the electromagnetic force is shown in figure 8(b).

Figure 8(b) shows that the secondary air gap has a remarkable influence on electromagnetic force. The force surface of the armature decreases as the secondary air gap increases. The optimum secondary air gap value in the range of 0.1mm-0.3mm is 0.1mm.



**Figure 8.** The secondary air gap and its effect on electromagnet force

### 3. ANALYSIS OF COIL TEMPERATURE FIELD OF ELECTROMAGNETIC PROPORTIONAL DIRECTIONAL VALVE

Research shows that one of the main failure forms of electromagnetic valve is coil overheating, resulting in coil burnout [13]. The Ohm heat of coil is the main heat source. The thermal conductivity and specific heat capacity of material are the important factors affecting the temperature field of coil. The temperature field of electromagnetic proportional directional valve varies in time and space and should be considered as a transient temperature field. Each of its periods can be regarded as steady state because the valve works intermittently. The heat transfer process of electromagnetic proportional directional valve mainly consists of heat conduction and convection heat transfer. It is a synthetical process of heat conduction and convection heat transfer.

The main internal heat of the electromagnet is heat conduction. The third order partial differential equation can be expressed as [14]:

$$\frac{\partial}{\partial t}(\rho c T) - \text{div}(\lambda \text{grad} T) = \ddot{q} \quad (3)$$

where,  $\rho$  -Material density,  $c$  -Material specific heat capacity,  $T$ -Temperature,  $\lambda$  -Material thermal conductivity,  $\ddot{q}$  -Heat generated by heat source in unit volume.

The first term of formula (3) is 0 if the steady-state temperature field is analyzed. Convection heat transfer in engineering applications can be calculated by the formula:

$$q = \alpha_{conv} \bullet A \bullet (T_0 - T_f) \quad (4)$$

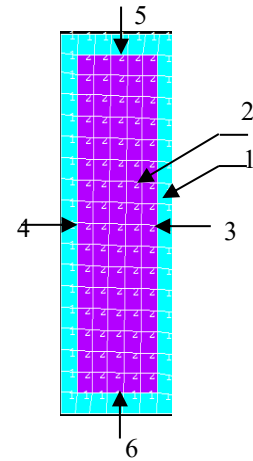
where,  $q$ -Heat flow,  $\alpha_{conv}$  -Convection heat transfer coefficient,  $A$ -Heat transfer area,  $T_0$  -Heat source temperature,  $T_f$  -Fluid temperature.

ANSYS thermal module is used to solve above equation.

(1) Pre-processing

The steady state temperature field of 2D is analyzed. The element type is PLANE55 and is axial symmetry [15]. The thermal conductivity 0.7 and 0.032 are set respectively for coil

and air [16]. The surface of the model is divided into quadrilateral free mesh, as shown in figure 9.



1-air; 2-coil; 3-outer surface; 4-inner surface; 5-upper surface; 6-lower surface

**Figure 9.** The coil meshing

(2) Loading two boundary conditions for the model

① Define heat density of the internal heat source:

$$Q_V = I^2 R / V_C \quad (5)$$

where,  $Q_V$  -The heat density,  $I$ -Coil current,  $R$ -Coil resistance,  $V_C$ -Coil volume.

The coil heat generation rate is set as [17]:

$$S = \frac{|J|^2}{\sigma} \quad (6)$$

where,  $S$ -Heat generation rate,  $\sigma$  -Coil conductivity,  $J$ -Coil current density.

In this paper, the parameters of the electromagnetic valve are set the same as formula (1).

② Loading natural convection heat transfer coefficient

Large space natural convection heat transfer coefficient is used on upper surface 5 and the limited space horizontal natural convection heat transfer coefficient is used on lower surface 6. The vertical space natural convection heat transfer

coefficient is used on outer surface 3 and the limited space vertical natural convection heat transfer coefficient is used on inner surface 4. The corresponding natural convection heat transfer coefficients of four surfaces are set in ANSYS as:

$$\lambda_{upper} = 12 \text{ W/m}^2 \cdot \text{K} \quad , \quad \lambda_{lower} = 4 \text{ W/m}^2 \cdot \text{K} \quad ,$$

$$\lambda_{outer} = 8 \text{ W/m}^2 \cdot \text{K} \quad , \quad \lambda_{inner} = 6 \text{ W/m}^2 \cdot \text{K} .$$

(3) The steady-state temperature analysis solver is used to solve the problem

(4) Post-processing, view the results of the solution

According to the formula (1) and formula (6), the factors that affect the coil heating include coil current, coil turn and coil geometry. The heat generation rate of the coil can be reduced by reducing the coil current, the number of coil turns and increasing the geometrical size of the coil, but decreasing the coil current and coil turns will also affect the electromagnetic force. As a result, the opening requirements of valve may not be reached, reducing its reliability. Therefore, coil temperature rise is studied from two aspects: the normal fluctuation of coil control current, the thermal conductivity of materials and the coefficient of convection heat transfer. The influence law is explored.

① The analysis results are opposite when the coil control current is 0.02A and 0.004A respectively.

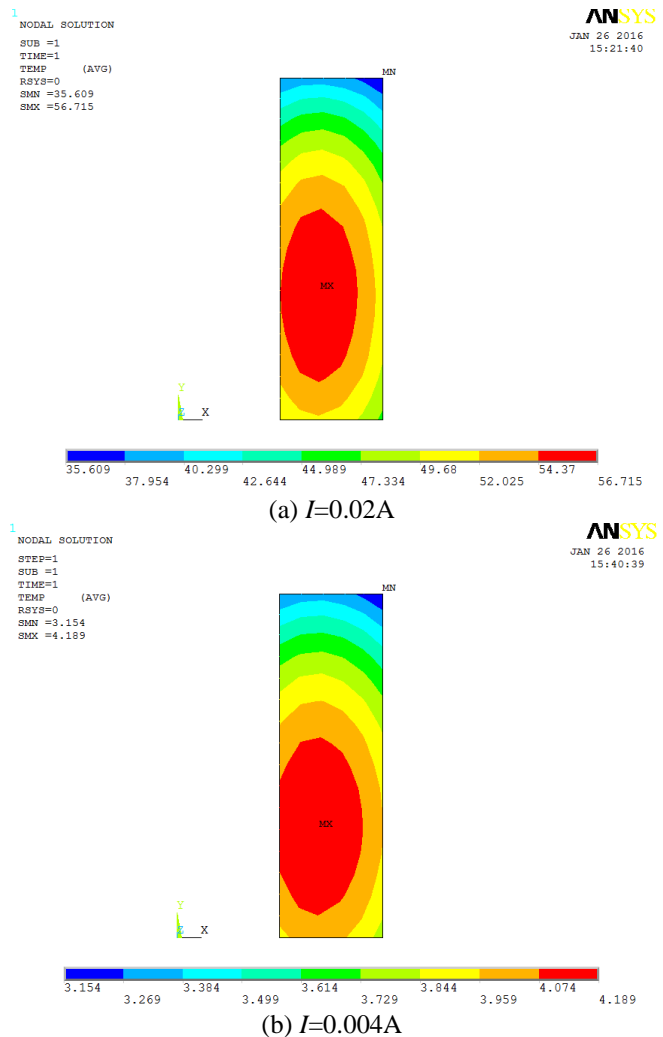


Figure 10. Coil temperature field distribution

The coil is made of copper wire with an electrical conductivity of  $5.9 \times 10^7 \text{ S/m}$ . The control current in the coil fluctuates between 0.004-0.02A when the valve works. The maximum temperature at the center of the coil is 4.189 degrees centigrade and there is almost no temperature rise compared with the lowest temperature 3.154 degrees of the coil edge, when the control current is 0.004A as shown in figure 10(b). On the other hand, the maximum temperature of the coil center is 56.715 degrees centigrade when the control current in the coil is 0.02°, as shown in figure 10(a). This can be explained by formula (5). The heat density of the inner heat source increases by square as the current increases and the heat energy increases, causing the coil temperature to rise. At the same time, the temperature at the center of the coil is higher than that at the edge because the heat source is in the center of the coil.

② The influence of coil thermal conductivity and convection heat transfer coefficient on coil temperature rise

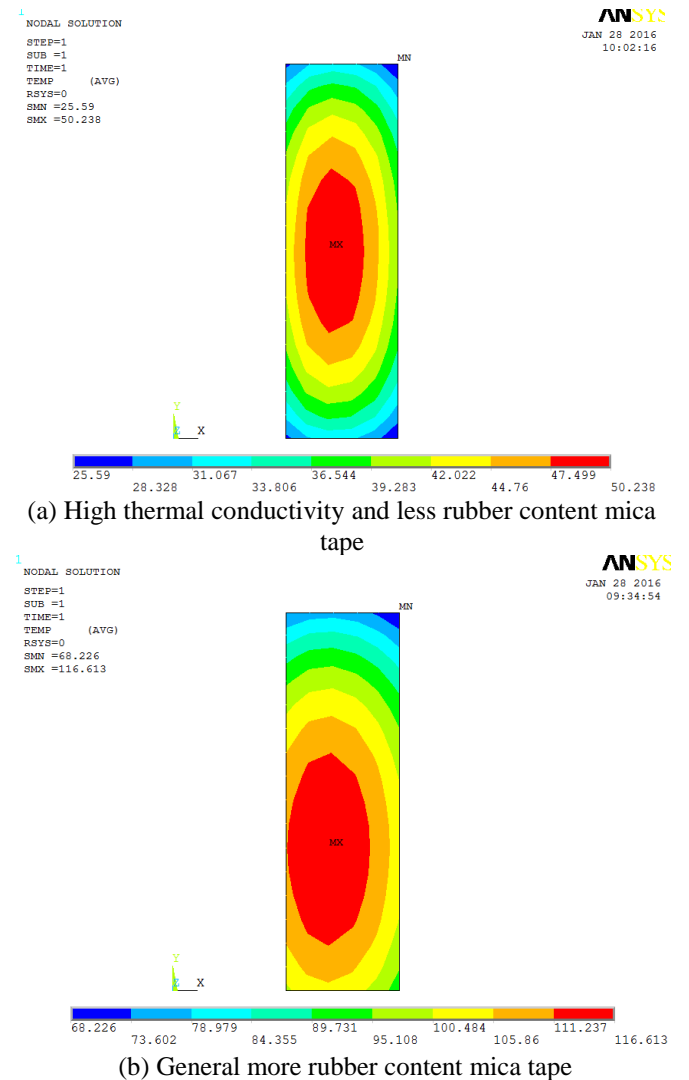


Figure 11. The comparison of coil temperature field distribution

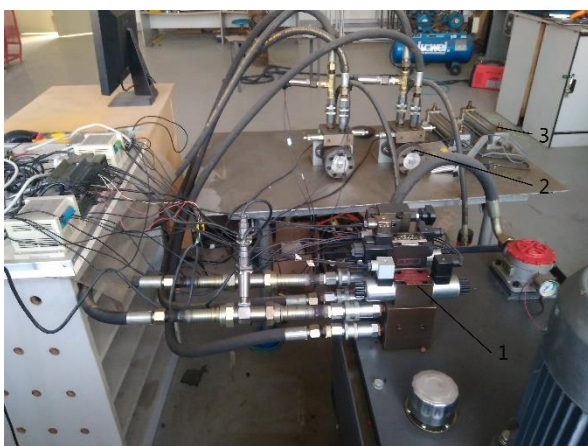
The thermal conductivity of the coil used in the previous analysis is a maximum value of 0.7, which is an ideal condition. In fact, the numerical value of the coil heat conduction coefficient is unknown and needs to be estimated and determined by the experimental results. In addition, the heat transfer coefficient of forced air convection increases up

to  $20 \text{ W/m}^2 \cdot \text{K}$  compared with the natural air convection. The thermal conductivity of the main insulation composed of different mica tapes can be measured by using the heat flux meter method [18, 19]. The results show that the thermal conductivity of insulation is proportionally increased with rubber material. The mica tape with high thermal conductivity and less rubber material can reach the highest thermal conductivity of  $0.327 \text{ W/m}^2 \cdot \text{K}$  at 130 degrees centigrade while the thermal conductivity of general mica tap with more rubber is  $0.294 \text{ W/m}^2 \cdot \text{K}$  at 130 degrees centigrade. The temperature changes in the forced air convection of the coils with two different thermal conductivity and main insulation are compared and analyzed, as shown in figure 11.

Figure 11 shows that the highest temperature in the center of the coil can be reduced from 116.613 degrees centigrade to 50.238 degrees centigrade using high thermal conductivity mica tape with less rubber as the main insulation material compared to general mica tap under the forced air convection (such as cooling fan) heat transfer condition. The cooling effect is obvious and temperature distribution of the coil is basically symmetrical along upper and lower surface and inner and outer surface.

#### 4. CONCLUSIONS

(1) Both the control current and the geometrical size of the electromagnet field have influence on electromagnetic force. First, coil control current, coil turns, the armature core length, rear angle and secondary air gap should be designed reasonably to ensure sufficient electromagnetic force to drive the spool and improve the reliability of the valve. Second, the electromagnetic proportional valve is a multi-physics field coupled system, including electromagnetic field, flow field and so on, so a multi-domain nonlinear dynamic model should be developed and used to predict the dynamic characteristics of the valve with multi-domain simulation software platform [20]. Moreover, the calculation of electromagnetic force should also consider the hydrostatic pressure, the spring force and damping force, in order to improve the accuracy.



1-Electromagnetic proportional directional valve; 2-Hydraulic motor; 3-Hydraulic cylinder

**Figure 12.** Hydraulic driven test bench of intelligent flexible sprayer chassis

(2) The coil temperature rise of the valve is one of the key factors that affect its reliability. The coil temperature rise is

mainly affected by the coil control current, the material thermal conductivity and the heat transfer coefficient. The valve used in this paper is not suitable for working full load current (0.02A) for a long time. Otherwise, the coil temperature rises and is easy to burnout. The forced air convection is better than the natural convection heat transfer and the coil has better heat dissipation effect. In addition, high thermal conductivity mica tape with less rubber is used as main insulation materials and the temperature rise of the coil is obviously lower than that of the general mica tape. The temperature can be decreased from 116.613 degree centigrade to 50.238 degree centigrade, which is beneficial to improve the reliability of the electromagnetic proportional directional valve.

(3) Theoretical reference is given for the reliability optimization design of the electromagnetic proportional directional valve. The valve optimized was used in the hydraulic driven test bench of intelligent flexible sprayer chassis. The speed of the hydraulic motor and hydraulic cylinder could be adjusted and controlled effectively by the valve, figure12 shows the hydraulic circuit.

#### ACKNOWLEDGEMENT

This work is supported by the scientific research project of Anhui Provincial Education Department (grant number KJ2017A508), by Stable Talent Project of Anhui Science and Technology University (grant number JXWD201701) and Anhui excellent young talents supporting program project (grant number gxypZD2018063).

The author declares that there is no conflict of interest regarding the publication of this paper.

#### REFERENCES

- [1] Cai W, Zheng XL, Zhang ZL, Huang XX. (2011). Failure mechanism analysis and transient characteristic simulation of hydraulic electromagnetic valve. *Chinese Journal of Scientific Instrument* 32(12): 2726-2733.
- [2] Liang FB, Li DT, Hu LF, Liu LB. (2005). Simulation of the high-speed powerful solenoid valve in a high-pressure common-rail injection system for diesel engine. *Transactions of the Chinese Society of Agricultural Machinery* 36(2): 8-11.
- [3] Lee GS, Sung HJ, Kim HC. (2012). Multi-physics analysis of a linear control solenoid valve. *Journal of Fluids Engineering* 135(1): 279-284.
- [4] Sun BB, Gao S, Ma C, Li JW. (2018). System power loss optimization of electric vehicle driven by front and rear induction motors. *International Journal of Automotive Technology* 19(1): 121-134. <http://dx.doi.org/10.1007/s12239-018-0012-5>
- [5] Lu X, Liu Z, Lu Z. (2017). Optimization design and experimental verification of track nonlinear energy sink for vibration control under seismic excitation. *Structural Control & Health Monitoring* (5): e2033. <http://dx.doi.org/10.1002/stc.2033>
- [6] Zhou C, Liang RB, Zhang JL. (2017). Optimization design method and experimental validation of a Solar PVT cogeneration system based on building energy demand. *Energies* 10(9): 1281. <http://dx.doi.org/10.3390/en10091281>

- [7] Luo X, Wang M, Dai G, Chen X. (2017). A Novel technique to compute the revisit time of satellites and its application in remote sensing satellite optimization design. *International Journal of Aerospace Engineering* 2017(6): 1-9. <http://dx.doi.org/10.1155/2017/6469439>
- [8] Bayat F, Tehrani AF, Danesh M. (2012). Finite element analysis of proportional solenoid characteristics in hydraulic valves. *International Journal of Automotive Technology* 13(5): 809-816. <http://dx.doi.org/10.1007/s12239-012-0081-9>
- [9] Lin A, Liu ZZ, Zhao L. (2004). Magnetic field analysis and electromagnetic force calculation for electromagnetic valves based on finite element method. *Journal of Shandong University (Engineering Science)* 34(6): 27-31.
- [10] Li JS, Hu WH, Lin HT, Li HP. (2005). Simulation analysis on static performance of ep solenoid valves based on ansys. *China Railway Science* 26(5): 72-75.
- [11] Li YX, Zou KF, Ou Y, Guang Y, Ou DS. (2004). Finite element analysis of electromagnetic field and experimental study of high-speed solenoid for common rail injector. *Transactions of CSICE* 22(6): 549-554.
- [12] Meng F, Tao G, Zhang MR, Chen HY. Optimization design and analysis of high speed wet proportional solenoid valve. *ACTA Armmentarii* 35(5): 590-596.
- [13] Han W, Liu ZH, Hu LJ, Liu BJ. (2011). Study on temperature field math model of driving coil of electromagnetism drive. *Micromotors* 44(6): 15-19.
- [14] Huang LM, Chen DG, Zhang JS. (2003). Analysis of thermal field and transient thermal circuit of solenoid magnet by considering physical parameters as functions of temperatures. *Transactions of China Electro technical Society* 18(5): 27-31.
- [15] Cai B, Liu Y, Ren C, et al. (2012). Probabilistic thermal and electromagnetic analyses of subsea solenoid valves for subsea blowout preventers. *Strojniski Vestnik* 58(11): 665-672. <http://dx.doi.org/10.5545/sv-jme.2012.681>
- [16] Liu QF, Bo HL, Wang L. (2013). Analysis of temperature field of direct action solenoid valve. *Nuclear Techniques* 36(4): 040650-1- 040650-5.
- [17] Lin SY, Xu ZH. (2012). Simulation and analysis on the three-dimensional temperature field of ac solenoid valves. *Proceedings of the CSEE* 32(36): 156-164.
- [18] Zhu HY. (2014). Measurement of thermal conductivity of the main insulation of stator windings in the turbine generator. *Motor Technology* 8(2): 48-50.
- [19] Lin ZY, Chen XZ. (2011). Experimental determination and numerical simulation of the radial thermal conductivity of coils. *Mechanical and electrical engineering technology* 40(08): 79-82.
- [20] Liu YF, Dai ZK, Xu XY. (2011). Multi-domain modeling and simulation of proportional solenoid valve. *Journal of Central South University of Technology* 11(18): 1589-1594. <http://dx.doi.org/10.1007/s11771-011-0876-2>